On Chaotic Flow around the Kida Vortex

L.M. Polvani and J. Wisdom
Massachusetts Institute of Technology, Cambridge MA 02139

The ordinary accounts of this vortex
in no way prepared me for what I saw.

Edgar Allan Poe

The "Kida vortex," a two-dimensional elliptical patch of constant vorticity embedded in a uniform quadratic background shear flow, has recently been the subject of a number of studies (Kida 1981, Dritschel 1989a, Meacham *et al.* 1989). These have concentrated mostly on understanding the linear stability of this solution and its nonlinear evolution under perturbations. In this paper we report on a new and surprisingly interesting aspect of the Kida vortex: chaotic advection is induced by the vortex in the surrounding fluid over regions much larger than the vortex itself, even for relatively small values of the background shear.

We start by presenting the Kida solution and describing the possible behaviors. We then proceed to derive the equations of motion for a passive tracer advected by the velocity field of the Kida vortex, and present some Poincare sections. The growth of the chaotic regions is studied by applying simple resonance overlap ideas. We conclude with a discussion of the implications of this finding for our understanding of two-dimensional turbulent fields.

1. THE KIDA VORTEX

The flow induced by an elliptical region of constant vorticity embedded in a quadratic shear flow is an exact time-dependent nonlinear solution of the Euler equations in two dimensions (Kida 1981). The quadratic form of the background is interesting because it can be thought of as the beginning of a local Taylor series expansion of the complicated velocity field in which the vortex is located. Since a shear flow can be decomposed as the sum of a rotation ω and a strain s, the streamfunction associated with the background field can be written:

$$\Psi_B = (1/4)\ (\omega + s)\ x^2\ +\ (1/4)\ (\omega - s)\ y^2, \tag{1}$$

where (x, y) are inertial Cartesian coordinates; ω and s may be functions of time. The result of Kida (1981) is that an elliptical vortex patch embedded in (1) remains elliptical for all times. The flow field is then entirely determined by the aspect ratio λ of the ellipse (we have chosen the convention $0 < \lambda < 1$) and its orientation, specified by the angle φ between the x-axis and the major axis of the ellipse. The evolution of

λ and φ is governed by the following system:

$$\frac{d\varphi}{dt} = \Omega_K + \frac{1}{2}[\omega\ +\ s\ \Lambda\ \cos 2\varphi] \qquad \text{and} \qquad \frac{d\lambda}{dt} = -s\ \lambda\ \sin 2\varphi\ , \tag{2}$$

where $\Omega_K = \lambda/(1+\lambda)^2$ is the angular velocity of an elliptical vortex patch in the absence of shear (a Kirchhoff vortex), and $\Lambda = (1+\lambda^2)/(1-\lambda^2)$. All variables in (1) and (2) are non-dimensional, with time and length scales chosen so that the patch has vorticity 1 and area π. Although φ and λ are not canonically conjugate variables, (2) can be shown to be a Hamiltonian system, and trajectories in (φ, λ) space are integrable. Despite their apparent simplicity, (2) give rise to a rich variety of behaviors, even for the case of constant ω and s to which we hereinafter restrict our discussion. An example is illustrated in Figure 1, where the (φ, λ) orbits for the $\omega = -.2$ and $s = 0.1$ are plotted. Depending on their aspect ratio vortices either rotate or "librate" around stationary solutions.

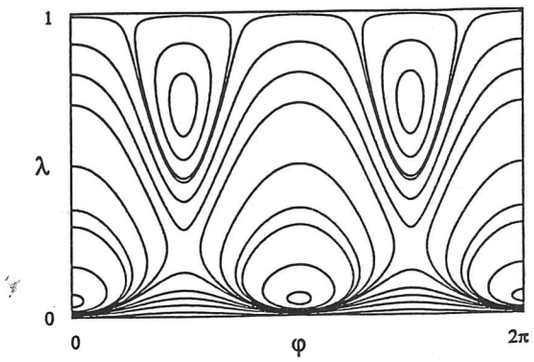

Figure 1: The (φ, λ) orbits for Kida vortices at $\omega = -0.2$ and $s = 0.1$, in region D of Figure 2.

Following Meacham *et al.*, it is simplest to classify the Kida solutions by dividing the (s, ω) parameter space into different regions, depending on the number of stationary solutions of (2); the latter were originally determined by Moore & Saffman (1971). Note first that (2) is invariant under the transformation $s \to -s$ and $\varphi \to \varphi + \frac{\pi}{2}$; thus only the $s > 0$ half-plane need be considered.

The whole phenomenology of the Kida solutions, synthesized in Figure 2, is physically understood as follows. For a given rotation ω, if the strain s is sufficiently large vortices of all aspect ratios will be sheared away: this is region C, where the only stationary solutions of (2) are for $\lambda = 0$. Conversely, for a given s all vortices will survive the straining provided the rotation is large enough, in either sense (these are regions A and E). In region B the rapidly rotating vortices (i.e. the more circular ones, c.f. the expression for Ω_K above) survive the straining although the background streamlines are hyperbolic, while the slow elongated vortices are sheared away. The richest behavior is found in region D, of which an example is given in Figure 1.

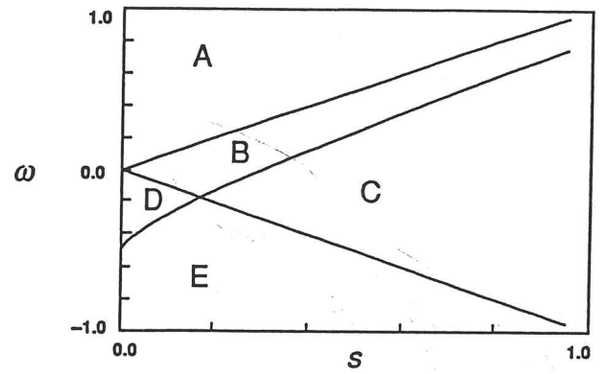

Figure 2: Phenomenology of the Kida solutions in the (ω, s) plane. The letters designate the regions described in the text.

The linear stability of the Kida solutions to two-dimensional normal mode perturbations has recently received much attention (Dritschel 1989a, Meacham *et al.* 1989). The essential result is the following: in addition to a Love-type instability similar to the one of the Kirchhoff vortex, resonance between the frequency of the (φ, λ) motion and the frequency of the disturbances on the elliptical boundary leads to a Mathieu-like parametric instability. However, the unstable bands become vanishingly thin and are associated with extremely small growth rates in the limit $s \to 0$. Moreover, the relevance of this linear analysis to the fully nonlinear evolution is unclear, since the instability often manifests itself only through the emergence of very thin filaments while the vortex retains its elliptical shape for long times. All results presented in this paper are for cases that are linearly stable.

2. CHAOTIC ADVECTION AROUND KIDA VORTICES

Having reviewed the Kida solutions from an *Eulerian* viewpoint, we now present new results regarding the *Lagrangian* motion of passive tracer advected by a Kida vortex. The total streamfunction $\Psi_T(x,y,t) = \Psi_B(x,y) + \Psi_V(x,y,t)$, is the sum of the quadratic background flow (1) and the streamfunction Ψ_V of a Kirchhoff vortex of aspect ratio $\lambda(t)$ and inclination $\varphi(t)$. In Cartesian coordinates, the position (x,y) of a particle evolves according to:

$$\frac{dx}{dt} = -\frac{\partial \Psi_T}{\partial y} \qquad \text{and} \qquad \frac{dy}{dt} = \frac{\partial \Psi_T}{\partial x}. \tag{3}$$

These are Hamilton's equations. The Hamiltonian Ψ_T contains explicit periodic time dependence, which suggests the presence of chaotic advection. Inside the vortex, however, Ψ_V is merely quadratic in x and y (Lamb 1945), so that (3) is linear with periodic coefficients; thus motion in the interior of the vortex is integrable.

To integrate (3) for the exterior field, we have found it easier to work in elliptical coordinates (ρ, ϑ) rotating and stretching with the vortex, since the analytical expression for Ψ_V is known in terms of ρ and ϑ, and there is no simple way of expressing (ρ, ϑ) in terms of (x,y). The conversion between the two coordinate systems, the

combination of an elliptical transformation and a rotation, is given by:

$$\begin{aligned} x &= c\,\cosh\rho\,\cos\vartheta\,\cos\varphi \;-\; c\,\sinh\rho\,\sin\vartheta\,\sin\varphi \\ y &= c\,\cosh\rho\,\cos\vartheta\,\sin\varphi \;+\; c\,\sinh\rho\,\sin\vartheta\,\cos\varphi, \end{aligned} \tag{4}$$

where $c^2 = (1-\lambda^2)/\lambda$ depends on time through λ. Substitution of (4) into (3) yields, after some algebra, the evolution equations for ρ and θ:

$$\begin{aligned} \frac{d\rho}{dt} &= \left(\frac{c^2h^2}{2}\right)\left[-\left(\Omega_K\,\sin 2\vartheta \;+\; 2c^{-2}\frac{\partial \Psi_V}{\partial \vartheta}\right) \;+\; \frac{1}{2}\,s\,\mathcal{F}(\rho,\vartheta,\varphi)\right] \\ \frac{d\vartheta}{dt} &= \left(\frac{c^2h^2}{2}\right)\left[-\left(\Omega_K\,\sinh 2\rho \;-\; 2c^{-2}\frac{\partial \Psi_V}{\partial \rho}\right) \;+\; \frac{1}{2}\,s\,\mathcal{G}(\rho,\vartheta,\varphi)\right], \end{aligned} \tag{5}$$

with

$$\begin{aligned} \mathcal{F} &= (\cosh 2\rho\,\sin 2\vartheta\,\cos 2\varphi + \sinh 2\rho\,\cos 2\vartheta\,\sin 2\varphi) \\ &\quad - \Lambda\,(\cos 2\varphi\,\sin 2\vartheta + \sinh 2\rho\,\sin 2\varphi) \\ \mathcal{G} &= (\sinh 2\rho\,\cos 2\vartheta\,\cos 2\varphi - \cosh 2\rho\,\sin 2\vartheta\,\sin 2\varphi) \\ &\quad + \Lambda\,(\sin 2\varphi\,\sin 2\vartheta - \sinh 2\rho\,\cos 2\varphi), \end{aligned}$$

and

$$c^2h^2 = \left(\cosh^2\rho \;-\; \cos^2\vartheta\right)^{-1}.$$

We have used a Bulirsch-Stoer algorithm to numerically integrate the autonomous 2-degree of freedom Hamiltonian problem constituted by (2) and (5), instead of solving (3) directly. Notice from (2) that for $s = 0$ the ellipse rotates at constant angular velocity with constant aspect ratio; in this case the Lagrangian fluid motion is integrable and, in the corotating frame, the streamlines are time-independent and appear as illustrated in Figure 3. It is important to note the presence of two saddle points S_1 and S_2 as well as two centers (usually referred to as 'ghost vortices'). For the weakly perturbed system, the chaotic zones are found to appear surrounding the separatrices (represented by the dotted lines in Figure 3), as is expected for weakly perturbed Hamiltonian systems.

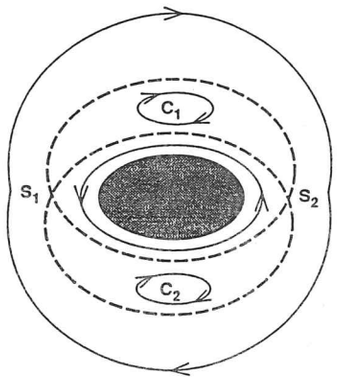

Figure 3: The Kirchhoff vortex streamfunction in the corotating frame. The solid lines are particles trajectories, the dashed lines are the separatrices, S_1 and S_2 the saddle points and C_1 and C_2 the 'ghosts'.

The important result of this study is that for small values of s and ω remarkably large chaotic zones are found surrounding the entire vortex. We show a typical example in Figure 4, were the surface of section for a Kida vortex at $\omega = -0.2$ and $s = 0.1$ is presented. The aspect ratio for this ellipse oscillates in the range $0.377431\ldots < \lambda < 0.9$. The figure is obtained by plotting a dot corresponding to the position of a single particle every period of the (φ, λ) motion, when $\varphi = 0$. In this and subsequent figures, the ellipse inside the chaotic zone coincides with the boundary of the vortex. We have found that chaotic zones are often very close to the vortex boundary. In view of this, it is not surprising that the behavior of vorticity filaments surrounding Kida vortices has been found to be extremely complicated (Dritschel 1989a). The presence of chaotic zones surrouding elliptical vortices may also provide an efficient mechanism for vortex stripping.

Another instance of great interest is the case $|\omega| = |s|$, for which the backround flow is a pure shear (an unbounded Couette flow) . The case $\omega = -s = 0.5$ is presented in Figure 5, for a vortex of aspect ratio $\lambda = 0.8$ at $\varphi = 0$. The chaotic zone appears to extend to arbitrarily large values of x, and is confined in y around the vortex. These results suggest that the elliptical vortices formed in unstable mixing layers may actually play a very important role in the mixing process.

To understand how the large chaotic regions emerge as the strength of the perturbing strain is increased, we have applied some simple ideas from the theory of overlapping resonances problem and found two main types of overlap that lead to large chaotic zones. The purpose of this analysis is by no means a detailed investigation of all the resonance overlaps in the Kida problem, but a simple approach that would account for the existence of large chaotic zones at small values of s and ω.

For case $\omega < 0$, one of the main resonances is associated with the 'ghost' of the exterior unperturbed Kirchhoff flow Ψ_V (see Figure 3), for which the period of the Lagrangian trajectory is identical to the period of the (φ, λ) motion; we designate this the 'Kirchhoff resonance'. The other main resonance is associated with the streamline pattern due to the superposition of the background quadratic shear with the equivalent monopolar velocity field of the vortex. We then consider the streamfunction Ψ_{pv} obtained by the superposition of a point vortex of strength π and the background flow (1), i.e. $\Psi_{pv} = (1/2)\ln r + \Psi_B$, where r is the radial distance from the origin. Such a streamfunction has an associated streamline pattern geometrically identical to the one shown in Figure 3, with the exception that it is rotated by $\pi/2$. The resonance of interest is the one associated with the 'ghost' vortex of Ψ_{pv}. It is a simple matter to find the radial distances r_{pv} and r_K of the resonances associated with Ψ_{pv} and Ψ_V (Polvani *et al.* 1989), and the respective half-widths Δr_{pv} and Δr_K, although the computation has to be performed numerically since transcendental equations need to be solved. According to the simple resonance overlap criterion we expect to observe large chaotic regions if

$$\Delta r_{pv} + \Delta r_K \; > \; r_{pv} - r_K \; . \tag{6}$$

As an illustration, the case $\omega = -0.1$ and $\lambda = 0.9$ is presented in Figure 6, where four surfaces of section are shown for increasing values of the perturbation

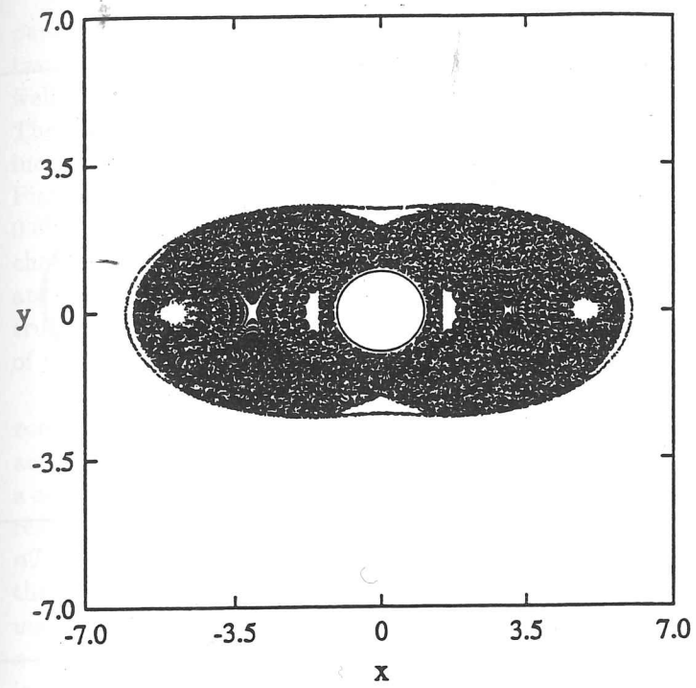

Figure 4: Surface of section for the Kida vortex at $\omega = -0.2$, $s = 0.1$ and $\lambda = 0.9$ at $\varphi = 0$. The figure was obtained with a single initial condition; 70,000 points are plotted. The aspect ratio varies in the interval $0.377431 < \lambda < 0.9$.

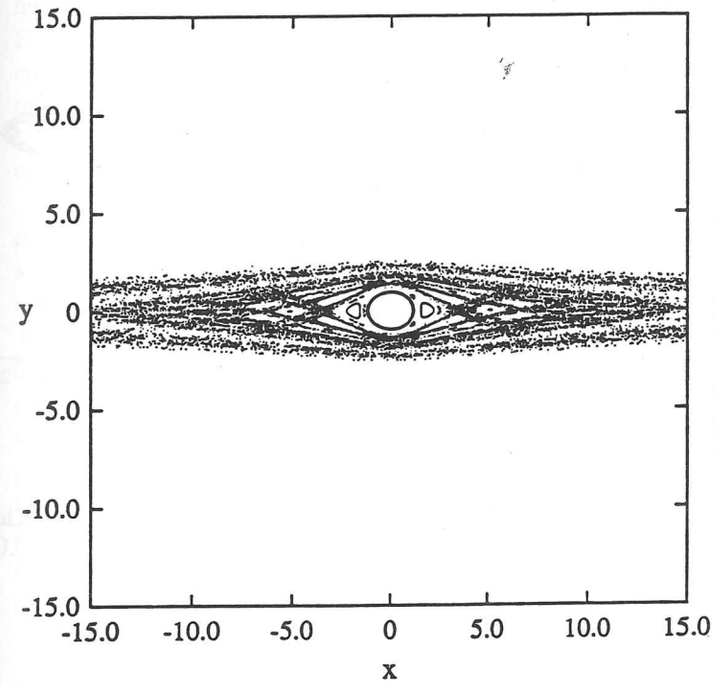

Figure 5: Surface of section for the Kida vortex at $\omega = 0.5$, $s = -0.5$ and $\lambda = 0.8$ at $\varphi = 0$. The background field is a simple shear flow of the form $u = (1/2)\,y$. The chaotic region appears to extend to arbitrarily large values of x . The aspect ratio for this vortex varies within $0.384535 < \lambda < 0.9$.

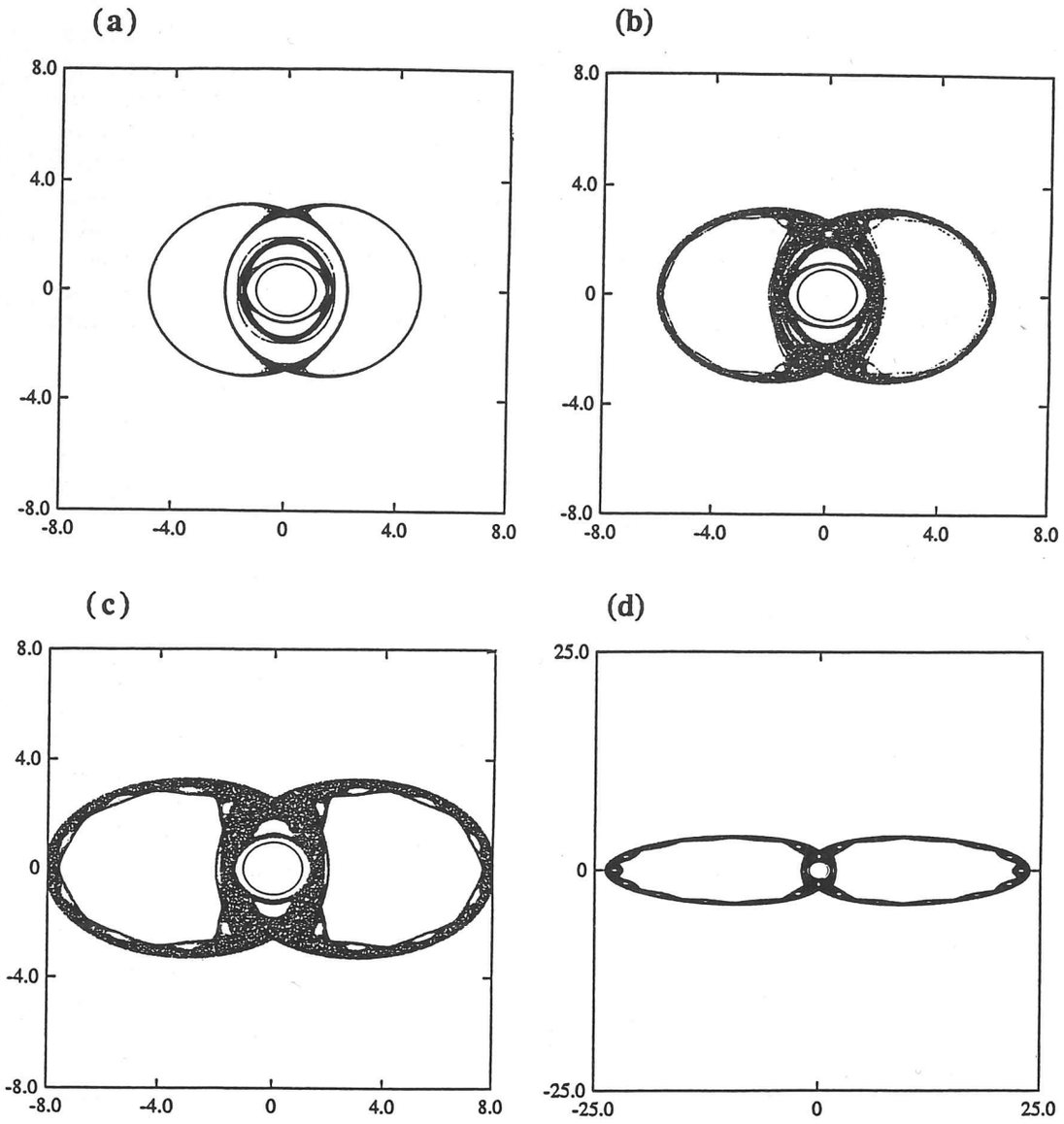

Figure 6: Surfaces of section at increasing values of the strain parameter s for Kida vortices at $\omega = -0.10$ and $\lambda = 0.9$ at $\varphi = 0$. (a) $s = 0.015$, (b) $s = 0.03$, (c) $s = 0.05$ and (d) $s = 0.09$. Each figure contains between 50,000 and 100,000 points.

parameter s. Resonance overlap occurs at $s = 0.0276$. At $s = 0.015$ (Fig. 6a) the two chaotic regions associated with the above mentioned resonances appear to be well separated. They have merged into a single chaotic zone at $s = 0.03$ (Fig. 6b). The transition compares favourably with the resonance overlap prediction (6). As increased the chaotic regions become larger. The section at $s = 0.05$ is shown in Figure 6c. It should be noted that the aspect ratio for this vortex varies in the range $0.696 < \lambda < 0.90$. This shows that even rather circular vortices may possess very large chaotic regions in the presence of extremely small straining fields. As the background approaches a pure shear (i.e. close to the line $|\omega| = |s|$), the chaotic zone becomes truly enormous (see Fig. 6d for the case $s = 0.09$), and are elongated in the direction of the shear.

When $\omega > 0$ the resonance associated with Ψ_{pv} cannot exist, and the large chaotic zones are produced by the overlap of resonances of the full Hamiltonian. Since the actual expansion of Ψ_T as a sum of resonances is rather complicated, we have preferred a simple numerical approach to determine both the location and width of the primary resonances. To the nth resonance, associated with the orbit that has a period $T_n = nT_{\varphi\lambda}$ (where $T_{\varphi\lambda}$ is the period of the (φ, λ) motion obtained from (2)), corresponds the frequency $\omega_n = \omega_{\varphi\lambda}/n$. To locate the resonances in the (x, y) plane we have used a Nelder-Mead scheme that minimizes the return distance on the section after n $T_{\varphi\lambda}$ periods. The frequency half-width $\Delta\omega_n$ associated with the nth resonance is determined by relating it to the frequency α_n of small oscillations around that resonance, which we compute by means of Floquet multipliers. Since the Kida vortex has a 4-fold symmetry, the nth resonance can be associated with a pendulum-like Hamiltonian of the form $H_n = \frac{1}{2}Ap^2 - B\cos(2n\vartheta - 2\omega_{\varphi\lambda}t)$, where p is canonically conjugate to the elliptical angle ϑ and zero at the resonance center. The actual values of A and B are immaterial. It is simple to show that for H_n the half-width Δw_n is related to α_n by the identity $\Delta\omega_n = \alpha_n/n$. Again we expect overlap when the simple criterion $(\Delta\omega_{n_1} + \Delta\omega_{n_2}) > (\omega_{n_1} - \omega_{n_2})$ is satisfied.

An example of this type of resonance overlap is given in Figure 7, where the surfaces of section for $\omega = 0$ and $\lambda = 0.5$ (at $\varphi = 0$) are shown at four values of s. At $s = 0.002$ (Fig. 7a) the chaotic regions associated with the Kirchhoff ($n = 1$) and $n = 2$ resonances are shown (50,000 points are plotted for each), and are not joined. The resonance overlap criterion predicts a value of $0.01 < s < 0.015$ for overlap. We find the $n = 1$ and $n = 2$ chaotic zones merge for s between 0.05 and 0.10; the latter case is shown in Figure 7b. The agreement with the resonance overlap prediction is satisfactory. In Figure 7c we have computed the chaotic regions for the first 7 primary resonances at $s = 0.02$; most of them are rather thin, and only the first two have merged (the figure contains approximately 300,000 points). Finally, the surface of section section for $s = 0.03$ (Fig. 7d) shows that most of them have by then fused into a single chaotic region; it is quite remarkable that the variations in aspect ratio and angular velocity for this vortex are very small, with $0.43525148\ldots < \lambda < 0.5$ and the a period differing from the Kirchhoff value by less than a half of one percent. Also of great interest is the fact that the chaotic zone is actually open (see the top of

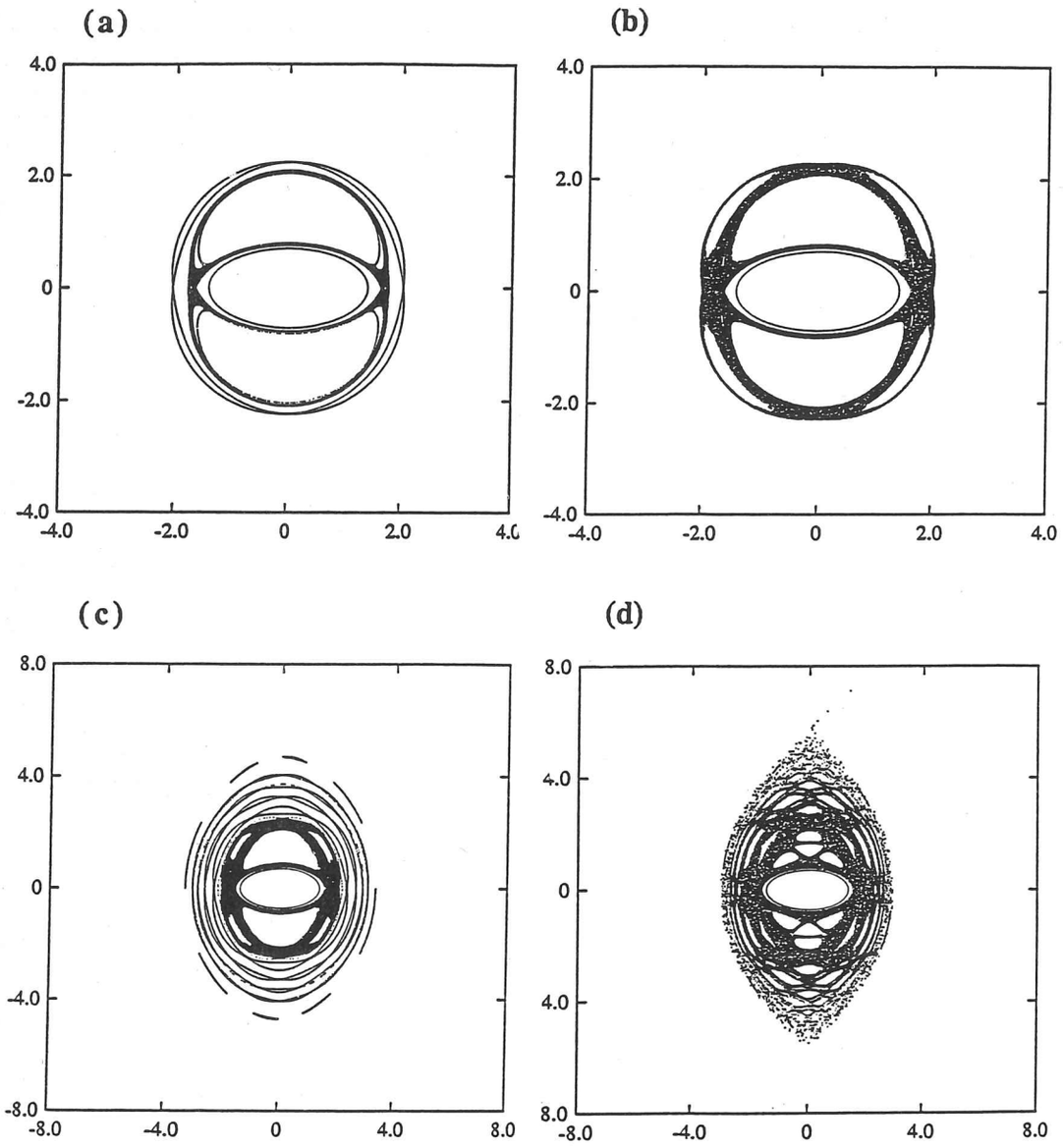

Figure 7: Surfaces of section at increasing values of the strain parameter s for Kida vortices at $\omega = 0$ and $\lambda = 0.5$ at $\varphi = 0$. (a) $s = 0.002$, (b) $s = 0.01$, (c) $s = 0.02$ and (d) $s = 0.03$. Notice that in (d) the particle actually escapes (see top of the figure) from the vicinity of the vortex.

Figure 7d), and the particle eventually escapes in the direction of the straining flow. In general we have found that for open chaotic zones, which exist only in region B of Figure 2, escapes occur very quickly (in a few $T_{\varphi\lambda}$ periods) unless $|\omega|$ is very close to $|s|$.

3. IMPLICATIONS FOR TWO-DIMENSIONAL TURBULENCE

Beyond their intrinsic value as the only presently known analytic nonlinear time-dependent solution of the Euler equations in two dimensions, Kida vortices are of great interest as the simplest model for the evolution of a vortex embedded in a complicated velocity field. This situation is encountered in high-Reynolds-number numerical simulations of two-dimensional turbulence, where strong isolated coherent vortices are known to emerge spontaneously from initially turbulent fields (McWilliams 1984). Recent results at very high resolution (Dritschel, 1989a) indicate that the vortices of 2D turbulence not only retain their ellipticity but are progressively stripped of the outer (lower) layers of vorticity, yielding elliptical structures with large vorticity gradients, for which a vortex patch is a reasonable first approximation.

In as much as the influence of the many distant vortices present in the field can be approximated by a uniform and constant quadratic shear, the discovery of very large chaotic zones surrounding Kida vortices suggests that the coherent structures of 2D turbulence may in fact be the *mixers* of the low levels of vorticity – which have been shown to behave not unlike a passive tracer (Babiano *et al.*, 1986). In particular, the results presented here for the Kida problem seem to provide a rationale for the recent observations of Benzi *et al.* (1988), who have discovered, in high-resolution spectral simulations of 2D turbulence, that the largest local exponential divergence of Lagrangian trajectories is found predominantly in the regions surrounding the coherent structures, while the motion in their interior is very stable.

Since the mixing we have described here is directly attributable to the dynamics of the homoclinic tangle (see, for instance, Rom-kedar *et al.* 1989) arising from the presence of hyperbolic points in the flow field surrounding the vortex, there is every reason to believe that similar behavior is generic to any two-dimensional vortex with a non-axisymmetric and time-dependent streamfunction. Among the many applications of interest, we would like to draw attention the stratospheric polar vortex, for which the advection of chemical tracers is a question of great current interest.

REFERENCES

BABIANO, A., BASDEVANT, C., LEGRAS, B. & SADOURNY, R. 1986 Vorticity and passive scalar dynamics in two-dimensional turbulence. *J. Fluid Mech.* **183**, 379-397.

BENZI, R. , PATERNELLO, S. & SANTANGELO, P. 1988 Self-similar coherent structures in two-dimensional decaying turbulence. *J. Phys. A* **21**, 1221-1237.

DRITSCHEL, D. 1989a The stability of elliptical vortices in an external straining flow. *J. Fluid Mech., sub judice.*

DRITSCHEL, D. 1989b Contour Dyamics and Contour Surgery. *Comp. Phys. Rep* **10**, 77-146.

KIDA, S. 1981 Motion of an elliptic vortex in a uniform shear flow. *J. Phys. Soc. Japan*, **50**, 3517-3520.

LAMB, Sir Horace, *Hydrodynamics*, Dover, N.Y.(1945).

MCWILLIAMS, J.C. 1984 The emergence of isolated coherent vortices in turbulent flow. *J. Fluid Mech.* **146**, 21-43.

MEACHAM, S.P., FLIERL, G.R. & SEND, U. 1989 Vortices in shear. To appear in *Dyn. Atoms. and Ocean.*

MOORE, D.W. & SAFFMAN, P.G. 1971 The structure of a line vortex in an imposed strain. In *Aircraft Wake Turbulence and its Detection*, p. 339, Plenum, N.Y. (1971).

POLVANI, L.M., FLIERL, G.R. & ZABUSKY, N.J. 1989a Filamentation of coherent vortex structures via separatrix crossing: a quantitative estimate of onset time. *Phys. Fluids A* **2**,181-184.

ROM-KEDAR, V., LEONARD, A. & WIGGINS, S. 1989 An analytical study of transport, mixing and chaos in an unsteady vortical flow. *J. Fluid Mech.*, submitted.